AIP Applied Physics Letters

Si(011) 16×2 gas-source molecular beam epitaxy: Growth kinetics

N. Taylor, H. Kim, P. Desjardins, Y. L. Foo, and J. E. Greene

Citation: Applied Physics Letters **76**, 2853 (2000); doi: 10.1063/1.126495
View online: http://dx.doi.org/10.1063/1.126495
View Table of Contents: http://scitation.aip.org/content/aip/journal/apl/76/20?ver=pdfcov
Published by the AIP Publishing

APPLIED PHYSICS LETTERS VOLUME 76, NUMBER 20 15 MAY 2000

Si(011)16×2 gas-source molecular beam epitaxy: Growth kinetics

N. Taylor, H. Kim, P. Desjardins, Y. L. Foo, and J. E. Greene[a]
Department of Materials Science, the Materials Research Laboratory, and the Coordinated Science Laboratory, University of Illinois, Urbana, Illinois 61801

(Received 19 November 1999; accepted for publication 20 March 2000)

The growth rates R_{Si} of Si layers deposited on Si(011)''16×2'' by gas-source molecular beam epitaxy from $\mathrm{Si_2H_6}$ were determined as a function of temperature T_s (400–975 °C) and $\mathrm{Si_2H_6}$ flux $J_{\mathrm{Si_2H_6}}(5.0\times10^{15}-9.0\times10^{16}\,\mathrm{cm^{-2}\,s^{-1}})$. R_{Si} ranges from 0.0015 μm h^{-1} at $T_s=400\,°\mathrm{C}$ to 0.415 μm h^{-1} at $T_s=975\,°\mathrm{C}$ with $J_{\mathrm{Si_2H_6}}=2.2\times10^{16}\,\mathrm{cm^{-2}\,s^{-1}}$. In the surface-reaction-limited regime at $T_s<725\,°\mathrm{C}$, R_{Si} initially exhibits an exponential decrease with $1/T_s$, then decreases at a slower rate at $T_s\leqslant550\,°\mathrm{C}$ as an additional deposition pathway becomes operative. In the impingement-flux-limited regime, $725\leqslant T_s\leqslant900\,°\mathrm{C}$, R_{Si} is independent of T_s but increases linearly with $J_{\mathrm{Si_2H_6}}$. At $T_s>900\,°\mathrm{C}$, $R_{\mathrm{Si}}(T_s)$ increases with T_s due to surface roughening. Overall, $R_{\mathrm{Si}}(J_{\mathrm{Si_2H_6}},T_s)$ is well described at $T_s\leqslant900\,°\mathrm{C}$ by a kinetic model incorporating two competing film growth mechanisms: (1) dissociative chemisorption of $\mathrm{Si_2H_6}$ onto dangling bonds followed by fast surface dissociation steps and second-order $\mathrm{H_2}$ desorption from the surface monohydride phase; and (2) $\mathrm{Si_2H_6}$ insertion into Si–H surface bonds followed by second-order desorption of $\mathrm{SiH_4}$. *© 2000 American Institute of Physics.* [S0003-6951(00)02320-2]

$\mathrm{Si_{1-x}Ge_x}(011)$ offers potential benefits over $\mathrm{Si_{1-x}Ge_x}(001)$ for certain types of device applications. The maximum film/substrate conduction-band offset in strained $\mathrm{Si_{1-x}Ge_xSi}(011)$ heterostructures is predicted to be substantially larger,[1] the optical band gap decreases more rapidly with increasing x,[1] and optical selection rules allow hole–intersubband transitions to be excited by light polarized parallel to $\mathrm{Si_{1-x}Ge_x/Si}(011)$ multiple quantum well layers.[2]

A major difference between Si(011) and Si(001), which has a significant effect on film growth kinetics and mechanistic rate limitations during gas-source film growth, is the considerably higher complexity of the Si(011) surface unit cell. Our previous results[3,4] confirmed published reports showing that the clean surface reconstruction is ''16×2.'' However, this surface, while labeled 16×2 based upon observed diffraction pattern periodicities, actually has a nonorthogonal

$$\begin{bmatrix} 17 & 1 \\ 2 & 2 \end{bmatrix}$$

structure with surface vectors $\overline{a}_s=17\overline{a}+\overline{b}$ and $\overline{b}_s=2\overline{a}+2\overline{b}$, where $\overline{a}=1/2[01\bar{1}]$ and $\overline{b}=[100]$.[3,4–6] The Si(011) surface reconstruction undergoes a gradual and reversible transformation from 16×2 to 1×1 at temperatures between 700 and 770 °C.[3,7,8] We showed, using $\mathrm{D_2}$ temperature programmed desorption (TPD), that the 16×2 reconstruction has a unit cell structure consisting of 16 adatom species and 8 π-bonded dimers, resulting in a maximum dangling bond coverage of 0.5 ML referenced to the 1×1 bulk surface.[3]

While the Si(011) surface structure has received significant attention, very little is known about the kinetics of Si(011) epitaxy. In this letter, we present the results of the first reported investigation of the temperature-and flux-dependent growth kinetics of Si(011) gas-source molecular beam epitaxy (GS-MBE) from $\mathrm{Si_2H_6}$.

All films were grown in a multichamber ultrahigh-vacuum (UHV) system, described in detail in Ref. 3, with a base pressure of 5×10^{-11} Torr. The system is equipped with provisions for TPD, reflection high-energy electron diffraction (RHEED), low-energy electron diffraction, and Auger electron spectroscopy (AES). The film growth experiments were carried out at temperatures $T_s=400-975\,°\mathrm{C}$ using $\mathrm{Si_2H_6}$ precursor fluxes $J_{\mathrm{Si_2H_6}}=5.0\times10^{15}-9.0\times10^{16}\,\mathrm{cm^{-2}\,s^{-1}}$. During deposition, the $\mathrm{Si_2H_6}$ molecular beam is delivered to the substrate through a directed tubular doser. The substrates were 0.5 mm thick B-doped Si(011) wafers ($3\times10^{17}\,\mathrm{cm^{-3}}$) with a miscut of 0.126° along ⟨112⟩.

Substrate cleaning consisted of solvent degreasing and wet chemical oxidation/etch cycles followed by an ultraviolet ozone treatment, UHV degassing, and oxide desorption.[3] RHEED patterns from substrates subjected to this procedure were sharp 16×2. No residual C or O was detected by AES.

Deposited Si film thicknesses were determined using secondary ion mass spectrometry and surface profilometry. The Cameca IMS-5F spectrometer was operated with a 10 keV $\mathrm{O_2^+}$ primary ion beam to detect $^{11}\mathrm{B}$ from the lightly doped substrates during sputter etching. Surface profilometry was then used to measure the depth of the crater. The uncertainty in film thickness is $\leqslant$ 4 nm.

All Si(011) layers exhibited sharp 16×2 RHEED patterns. $\mathrm{D_2}$ TPD spectra were obtained from Si(011)16×2 surfaces dosed for successively longer times to provide normalized coverages $\theta_{\mathrm{D}}/\theta_{\mathrm{D,sat}}$, where $\theta_{\mathrm{D,sat}}$ is the saturation coverage. The spectra are very similar to those we obtained from Si(111)[4] and consist of a low temperature desorption peak centered at 430 °C and a high temperature feature at 550 °C. The primary difference between the Si(011) and

---

[a] Author to whom correspondence should be addressed; electronic mail: greene@mrlxp2.mrl.uiuc.edu

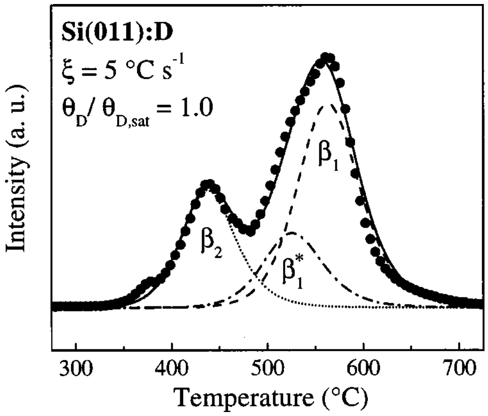

FIG. 1. Fitted (solid and dashed lines) and measured (filled circles) D_2TPD spectra from a Si(011) sample with $\theta_D/\theta_{D,sat}=1.0$. The linear heating rate in all experiments was 5 °C s^{-1}.

Si(111) TPD spectra is that the high-temperature Si(011) feature contains a more obvious shoulder peak, split in this case by 30 °C and centered at 520 °C. Following the procedure described in Refs. 3 and 4, we have fit the data using standard Polanyi–Wigner analyses. An example is shown in Fig. 1. The β_2 peak arises due to D_2 desorption from the dideuteride phase while the higher temperature β_1^* and β_1 peaks are associated with desorption from adatoms and rest atoms in the monohydride phase.[3,4] All peaks are second order and we have ignored the small feature near 375 °C, attributed to desorption from trideuteride species, since it is not relevant to the present Si(011) growth kinetics experiments. Frequency factors v and desorption activation energies E_d are $1\times10^{15}\,s^{-1}$ and 2.22 ± 0.02 eV for β_2, $2\times10^{15}\,s^{-1}$ and 2.55 ± 0.02 eV for β_1^*, and $2\times10^{15}\,s^{-1}$ and 2.68 ± 0.02 eV for β_1.[3,4]

The film growth rate R_{Si} as a function of T_s with $J_{Si_2H_6}=2.2\times10^{16}\,cm^{-2}\,s^{-1}$ is shown in Fig. 2. Over the temperature range between 550 and 900 °C, $R_{Si}(T_s)$ follows the general form expected for chemical vapor deposition in which R_{Si} decreases exponentially with $1/T_s$ at low temperatures in a surface-reaction-limited mode, while at high temperatures R_{Si} tends to saturation in an impingement-flux-limited mode. In the surface-reaction-limited growth mode, R_{Si} increases from 0.011 μm h^{-1} at 550 °C to 0.111 μm h^{-1} at 700 °C as layer growth proceeds by the second-order dissociative adsorption of Si_2H_6 onto dangling bonds whose coverage θ_{db} is determined by the associative desorption rate of H_2. The surface structural phase transition from 1×1 to 16×2, which for Si(011) occurs near 700 °C, does not have a significant effect on the shape of $R_{Si}(T_s)$.[9] At $T_s>725$ °C, the steady-state hydrogen coverage on the 1×1 reconstructed Si(011) surface is sufficiently low ($\theta_H<0.19$ ML) that R_{Si} is limited primarily by the Si_2H_6 impingement rate. With $J_{Si_2H_6}=2.2\times10^{16}\,cm^{-2}\,s^{-1}$, $R_{Si}\simeq0.21\,\mu m\,h^{-1}$ at $725\leqslant T_s\leqslant900$ °C. The increase in R_{Si} at $T_s>900$ °C is due to surface roughening as observed by RHEED, resulting in a higher surface area and a change in the overall Si_2H_6 sticking probability due to orientation dependence.

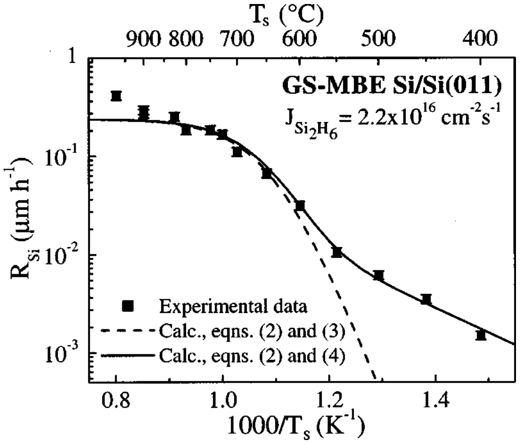

FIG. 2. Experimental and calculated Si(011) growth rates R_{Si} as a function of temperature T_s for an incident Si_2H_6 flux $J_{Si_2H_6}=2.2\times10^{16}\,cm^{-2}\,s^{-1}$.

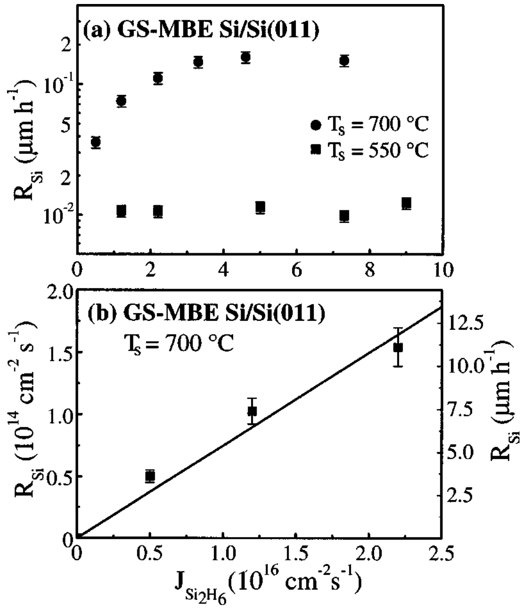

FIG. 3. (a) Log–log plots of Si(011) growth rates R_{Si} as a function of the incident Si_2H_6 flux $J_{Si_2H_6}$ at $T_s=550$ and 700 °C. (b) $R_{Si}(cm^{-2}\,s^{-1})$ vs $J_{Si_2H_6}$ at $T_s=700$ °C.

At $T_s\leqslant550$ °C, a new surface reaction pathway becomes operative and R_{Si} grows progressively larger than values predicted by a single exponential dependence on $1/T_s$. As discussed below, we propose that this is due to R_{Si} becoming increasingly controlled by direct insertion of Si_2H_6 into Si–H surface bonds.

Figure 3(a) is a plot of R_{Si} as a function of Si_2H_6 flux during film growth in the surface-reaction-limited regime ($T_s=550$ °C) and in the transition region ($T_s=700$ °C). The steady-state H coverage θ_H, obtained from using Eq. (2) below and noting that $(\theta_{db}+\theta_H)=1$ ML, is 0.87 ML at $T_s=550$ °C and only 0.26 at $T_s=700$ °C for $J_{Si_2H_6}=2.2\times10^{16}\,cm^{-2}\,s^{-1}$. R_{Si} at $T_s=550$ °C remains constant at $0.011\pm0.001\,\mu m\,h^{-1}$ and is not a function of $J_{Si_2H_6}$ since film growth in this regime is controlled by the H_2 desorption rate rather than the precursor dosing rate. In contrast, R_{Si} at 700 °C initially increases linearly with $J_{Si_2H_6}$, typical of flux-limited growth, before saturating at a value of 0.153 $\pm0.006\,\mu m\,h^{-1}$ with $J_{Si_2H_6}\geqslant3.3\times10^{16}\,cm^{-2}\,s^{-1}$. Thus, θ_H increased sufficiently at the higher fluxes, due to competition between Si_2H_6 adsorption and H_2 desorption, to drive the growth kinetics into the surface-reaction-limited regime.

We have previously demonstrated that $R_{\mathrm{Si}}(J_{\mathrm{Si_2H_6}},T_s)$ for GS-MBE deposition from $\mathrm{Si_2H_6}$ on the much simpler Si(001)2×1 (Ref. 10) surface can be well described by a model, containing no fitting parameters, in which second-order dissociative chemisorption of $\mathrm{Si_2H_6}$ is followed by a series of fast surface decomposition reactions with the final step being first-order $\mathrm{H_2}$ desorption from the surface monohydride phase. However, our TPD results for Si(011) show that $\mathrm{Si_2H_6}$ adsorption and $\mathrm{H_2}$ desorption are both second order.[3,4] Thus, making the reasonable assumption that the intermediate surface reaction steps are also fast on Si(011), the overall change in θ_{db} during Si(011) GS-MBE is given by the expression

$$\frac{d\theta_{\mathrm{db}}}{dt}=-2J_{\mathrm{Si_2H_6}}k_a\theta_{\mathrm{db}}^2+k_d(1-\theta_{\mathrm{db}})^2. \tag{1}$$

The reaction rate constant k_a for $\mathrm{Si_2H_6}$ adsorption on Si(011) can be expressed as $S_{\mathrm{Si_2H_6}}/N_s$ in which $S_{\mathrm{Si_2H_6}}$ is the zero-coverage reactive sticking probability and N_s is the bulk surface site number density, $9.6\times10^{14}\,\mathrm{cm^{-2}}$. k_d in Eq. (1) is the recombinative $\mathrm{H_2}$ desorption rate constant which can be expressed as $\nu\cdot\exp(E_d/kT_s)$, where the frequency factor $\nu=2\times10^{15}\,\mathrm{s^{-1}}$ and the desorption activation energy $E_d=2.68\,\mathrm{eV}$ are known from the β_1 TPD results discussed above. $S_{\mathrm{Si_2H_6}}$ at 700 °C was determined from the slope of the R_{Si} vs $J_{\mathrm{Si_2H_6}}$ data in Fig. 3(b) to be 0.0075, approximately 20% of the Si(001) value.[10] We assume, as in the case for Si(001) GS-MBE from $\mathrm{Si_2H_6}$,[11] that $S_{\mathrm{Si_2H_6}}$ for Si(011) is not strongly T_s dependent.

The steady-state dangling bond coverage obtained from Eq. (1) is

$$\theta_{\mathrm{db}}=\left[1+\left(\frac{2I_{\mathrm{Si_2H_6}}S_{\mathrm{Si_2H_6}}}{N_s\nu\exp(-E_d/kT_s)}\right)^{0.5}\right]^{-1} \tag{2}$$

and the film growth rate is given by

$$R_{\mathrm{Si}}=\frac{2J_{\mathrm{Si_2H_6}}S_{\mathrm{Si_2H_6}}\theta_{\mathrm{db}}^2}{N}, \tag{3}$$

in which N is the bulk Si atom number density, $5\times10^{22}\,\mathrm{cm^{-3}}$. In the flux-limited regime where θ_{db} approaches its saturation value, Eq. (3) predicts R_{Si} to be nearly independent of T_s and to increase linearly with $J_{\mathrm{Si_2H_6}}$, as observed in Fig. 3(b).

The dashed curve in Fig. 2 is a plot of R_{Si} vs T_s based upon Eqs. (2) and (3). While it provides a good fit to the data for the growth temperature range $550<T_s\leqslant900\,^\circ\mathrm{C}$, experimental R_{Si} values are higher than predicted at both higher and lower temperatures. The difference at higher temperatures is due to surface roughening.

The $R_{\mathrm{Si}}(T_s)$ results at $T_s\leqslant550\,^\circ\mathrm{C}$ indicate that a new reaction path for film growth becomes competitive with the mechanism described by Eqs. (2) and (3). Dangling bond coverages determined by TPD range from 0.133 ML at 550 °C to 0.002 ML at 400 °C. At these temperatures, where θ_{H} is high and approaching saturation, we propose that film growth via the direct insertion of incident $\mathrm{Si_2H_6}$ molecules into Si–H surface bonds becomes significant. A similar pathway has been suggested by Kulkarni *et al.*[11] and Boland[12] to contribute to low-temperature Si(111) and Si(001) growth, respectively. Two of the three monohydride adatom backbonds on the Si(011) 16×2 surface are highly strained and easily broken during $\mathrm{H_2}$ adsorption to form dihydride species.[3,4] By analogy, we propose that the backbonds are also attacked by $\mathrm{Si_2H_6}$, resulting in bond breakage and the insertion of a $\mathrm{SiH_2}$ fragment accompanied by $\mathrm{SiH_4}$ desorption. This results in the addition of a second term to Eq. (3),

$$R_{\mathrm{Si}}=\frac{2J_{\mathrm{Si_2H_6}}S_{\mathrm{Si_2H_6}}\theta_{\mathrm{db}}^2}{N}+\frac{2J_{\mathrm{Si_2H_6}}S_{\mathrm{Si_2H_6}}^{\mathrm{Si-H}}\theta_{\mathrm{H}}}{N}. \tag{4}$$

$S_{\mathrm{Si_2H_6}}^{\mathrm{Si-H}}$ is the $\mathrm{Si_2H_6}$ reactive sticking probability via insertion, a thermally activated process with activation energy $E_{\mathrm{Si-H}}$. Figure 2 shows that calculated results based on Eqs. (2) and (4) exhibit very good agreement with experimental data over the entire growth temperature range until surface roughening becomes significant at $T_s>900\,^\circ\mathrm{C}$. The best fit shown by the solid line in Fig. 2 gives $E_{\mathrm{Si-H}}=0.5\,\mathrm{eV}$ which yields $S_{\mathrm{Si_2H_6}}^{\mathrm{Si-H}}$ values varying from 5.24×10^{-4} at 550 °C to 1.09×10^{-4} at 400 °C.

In conclusion, the $R_{\mathrm{Si}}(T_s)$ data are well described by a kinetic model incorporating two competing film growth mechanisms: (1) dissociative chemisorption of $\mathrm{Si_2H_6}$ onto dangling bonds followed by fast surface dissociation steps and second-order $\mathrm{H_2}$ desorption from the surface monohydride phase; and (2) $\mathrm{Si_2H_6}$ insertion into Si–H surface bonds followed by second-order desorption of $\mathrm{SiH_4}$.

The authors acknowledge the financial support of the SRC and the Materials Science Division of the US Department of Energy (DOE) under Award No. DEFG02-ER9645439. P.D. is partially supported by NSERC of Canada. The authors also appreciate the use of the Center for Microanalysis of Materials at the University of Illinois, which is partially supported by the DOE.

[1] C. W. Liu, J. C. Sturm, Y. R. J. Lacroix, M. L. W. Thewalt, and d. D. Perovic, Appl. Phys. Lett. **65**, 76 (1994).

[2] T. L. Kreifels, R. L. Hengehold, Y. K. Yeo, P. E. Thomson, and D. S. Simons, J. Vac. Sci. Technol. A **13**, 636 (1995).

[3] N. Taylor, H. Kim, T. Spila, J. A. Eades, G. Glass, P. Desjardins, and J. E. Greene, J. Appl. Phys. **85**, 501 (1999).

[4] H. Kim, N. Taylor, T. Spila, G. Glass, S. Y. Park, J. E. Greene, and J. R. Abelson, Surf. Sci. **380**, L496 (1997).

[5] S. Miura, K. Kato, T. Ide, and T. Ichinokawa, Surf. Sci. **191**, 259 (1987).

[6] E. J. van Loenen, D. Dijkkamp, and A. J. Hoeven, J. Microsc. **152**, 487 (1988).

[7] G. Shimaoka, Appl. Surf. Sci. **65/66**, 569 (1993).

[8] Y. Yamamoto, T. Sueyoshi, T. Sato, and M. Iwatsuki, Jpn. J. Appl. Phys., Part 2 **32**, L532 (1993).

[9] The effect of the surface phase transformation on R_{Si} is difficult to observe since it occurs over a narrow temperature range in the flux-limited to surface-reaction-limited transition region. However, we know from TPD results that $\theta_{\mathrm{db}}(1\times1)=2\,\theta_{\mathrm{db}}(16\times2)$. Thus, the $R_{\mathrm{Si}}(T_s)$ data suggest that the $\mathrm{Si_2H_6}$ reactive sticking probability is lower on the 1×1 than on the 16×2 reconstructed surface.

[10] T. R. Bramblett, Q. Lu, T. Karasawa, M.-A. Hasan, S. K. Jo, and J. E. Greene, J. Appl. Phys. **76**, 1884 (1994).

[11] S. K. Kulkarni, S. M. Gates, B. A. Scott, and H. H. Sawin, Surf. Sci. **239**, 13 (1990); S. K. Kulkarni, S. M. Gates, C. M. Greenlief, and H. H. Sawin, *ibid.* **239**, 26 (1990).

[12] J. J. Boland, Phys. Rev. B **44**, 1383 (1991).